

Ordered stripes to crack patterns in dried particulates of DNA coated gold colloids via modulating nanoparticle-substrate interactions

Suman Bhattacharjee^{†,‡} and Sunita Srivastava^{*,‡}

[†]*Centre for Research in Nanotechnology & Science (CRNTS), Indian Institute of
Technology Bombay, Mumbai-400 076, India*

[‡]*Soft Matter and Nanomaterials Laboratory, Department of Physics, Indian Institute of
Technology Bombay, Mumbai-400 076, India*

E-mail: sunita.srivastava@phy.iitb.ac.in

Phone: +91-22-2576-7572

Supplementary Information

DNA chain sequence

The thiol (-SH) terminated DNA chains of 50 bases were used for surface functionalization of the gold nanoparticle via SH-Au chemistry as discussed in main text. The DNA chain sequence is as below:

5'-/5ThioMC6-TTTTTTTTTTTTTTCGTTGGCTGGATAGCTGTGTTCTTAA
CCTAACCTTCAT-3'

Particle system characterization

UV-Vis spectroscopy

UV-visible spectroscopy is done to verify the functionalization of AuNP with DNA. Absorbance spectra of AuNP with (red) and without DNA (black) is shown here in Fig.S1. 15nm AuNP shows a peak at 519nm. Red shift in DNA-AuNP LSPR peak suggests increase in size due to DNA functionalization and the hump at 260nm confirms the existence of DNA in the sample. Calculation for concentration of DNA-AuNP is done using Beer-Lambert's law.¹ Value of extinction coefficient for 15nm AuNP is assumed to be $3.64 \times 10^8 M^{-1}cm^{-1}$.

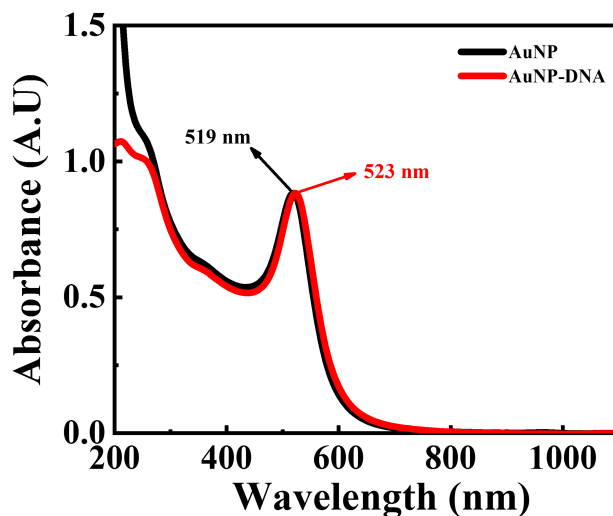


Fig. S1: UV-Visible spectroscopy data for AuNP and DNA-AuNP.

Dynamic Light Scattering (DLS)

Hydrodynamic size (Fig. S2) and zeta potential (Fig. S3) of the AuNP and DNA-AuNP system are measured using the DLS method. For AuNP hydrodynamic size is $\sim 18.7nm$ and zeta potential is $\sim -22.5mV$ owing to citrate capping around the particles. After functionalization, hydrodynamic size becomes $\sim 59.2nm$ and zeta potential is $\sim -56.6mV$. A difference of $\sim 40.5nm$ between AuNP and DNA-AuNP hydrodynamic size suggests a $\sim 20nm$ long DNA chain attached to the particles along with the higher negative zeta potential for DNA's charge.

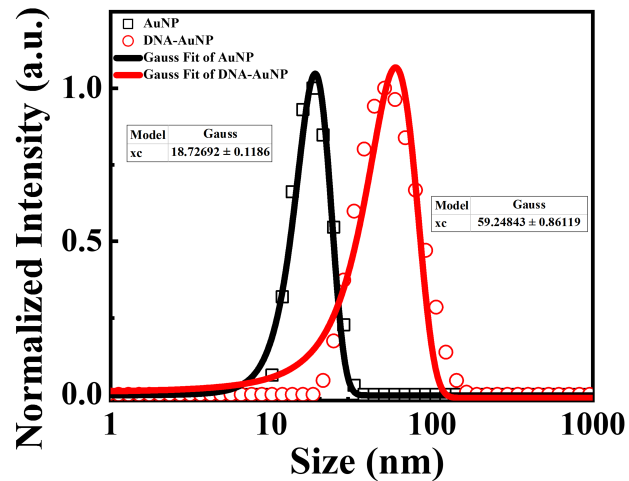


Fig. S2: DLS for AuNP and DNA-AuNP to estimate hydrodynamic size of the particles. x_c denotes the mean hydrodynamic size of the particles.

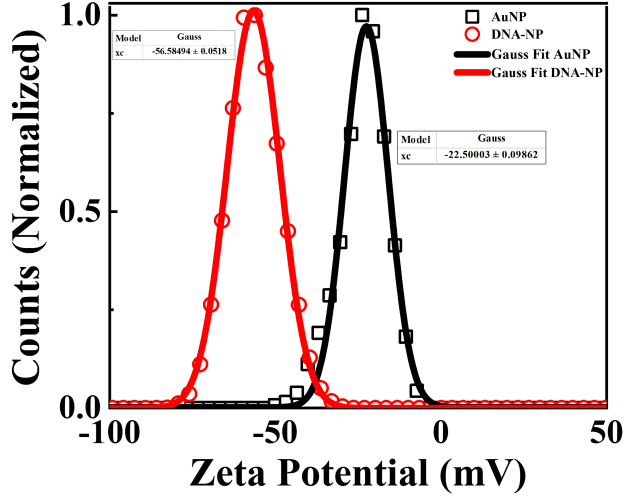


Fig. S3: Zeta potential estimation for AuNP and DNA-AuNP solution. x_c denotes the values for each system.

Substrate characterization

Contact angle Surface free energy (SFE) measurement

Using Neumann's equation,² SFE is calculated for SiO_2 surface. The parameters used in the measurement is given below in Table S1. $\beta = 0.0001247$ is assumed here according to experimental analysis by Li and Neumann,³ to make the surface energy calculation independent of liquid.

Table S1: Values for different parameters for the calculation of surface energy of SiO_2 substrate.

Parameters/Systems	Water	EG	DIM
γ_{lv} (mN/m)	72.8	48	50.8
Contact angle(°)	73.0 ± 2.1	47.1 ± 3.4	53.5 ± 1.9
γ_{sv} (mN/m)	39.9 ± 1.3	35.3 ± 1.5	34.5 ± 0.9

Atomic Force Microscopy (AFM) imaging

AFM imaging was done on freshly cleaned Si and SiO_2 surfaces to check on roughness and homogeneity as shown in Fig.S4. Roughness is calculated based on the straight line drawn on the image. From the height profile of the lateral, mean deviation of the maximas

and minimas are taken as roughness value and it is $\sim 0.8nm$ for both cases which can be considered negligible.

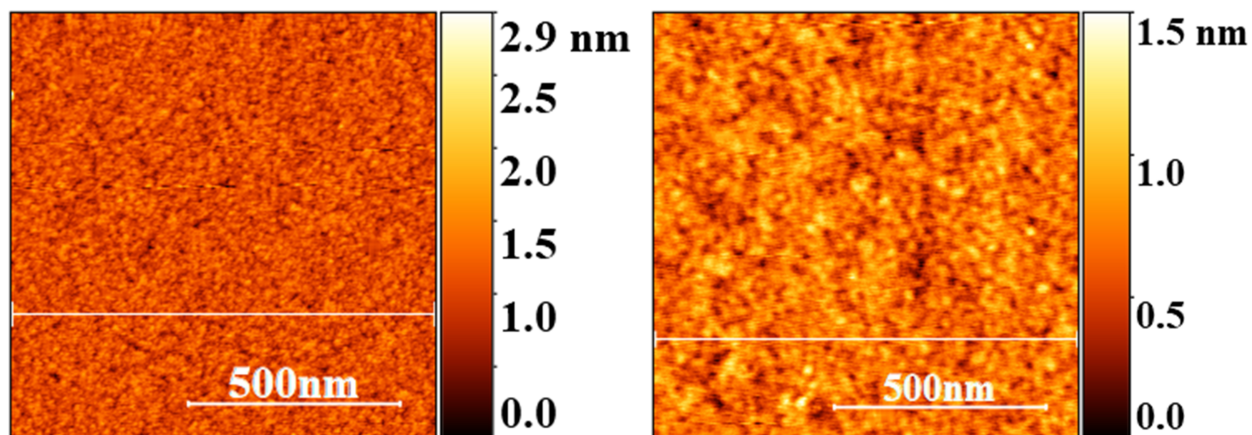


Fig. S4: AFM images for Si (left) and SiO_2 (right) substrates.

Profilometer measurements on dried patterns

Profilometer scans on coffee ring patterns were done to compare with the SEM micrograph analysis. Fig.S5 shows a radial scan from the outside of coffee ring pattern (from substrate) to inside the ring. The Gaussian profile indicates the coffee ring while higher height on the inside part of ring signifies particle deposition. For a sample of $5\mu L$ and $12.5nM$ system, CRW obtained from SEM image is $\sim 24\mu m$ and from the FWHM of the fitted graph in Fig.S5, it is $24.4 \pm 0.1\mu m$. Maximum height of deposition is about $\sim 1264nm$ which approximately suggests ~ 84 layers of DNA-AuNP stacked vertically on the coffee ring.

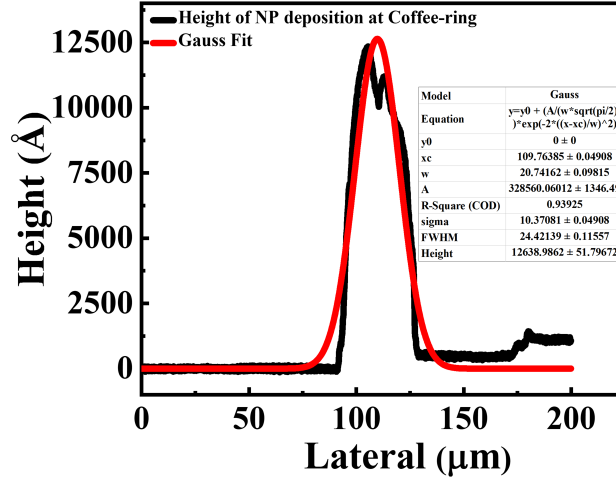


Fig. S5: Profilometer scan (edge to centre) on self-assembled DNA-AuNP structure.

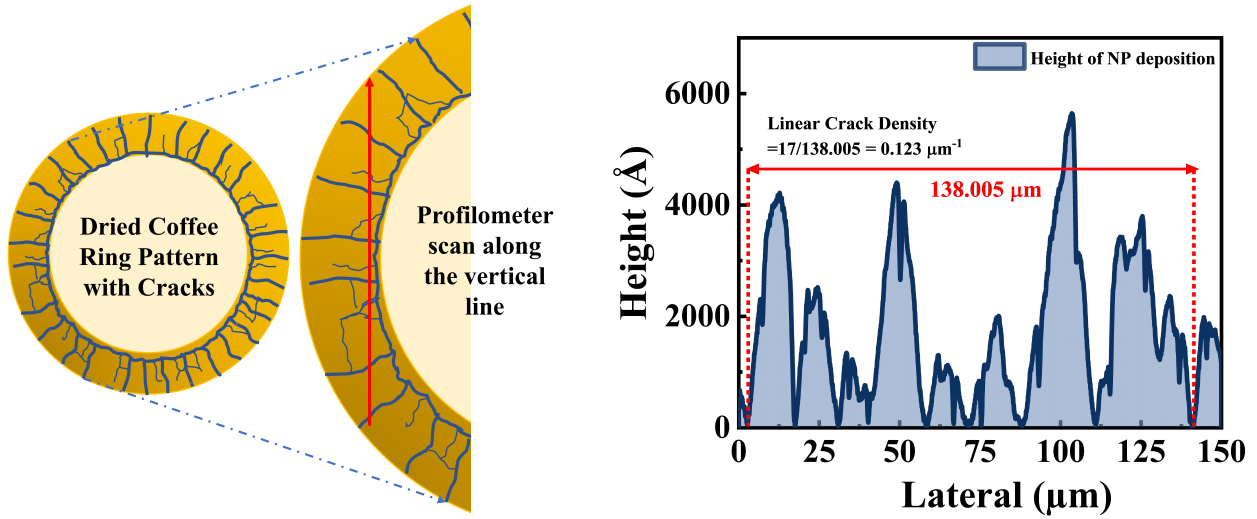


Fig. S6: Schematic showing profilometer scan along the coffee ring to verify the existence of cracks. The dips in particle deposition height as seen in the Height vs Lateral plot suggest that cracks are present.

A profilometer scan along the arc of a coffee ring (small portion of arc can be considered a straight line) is done to identify the cracks (Fig.S6). Approximately 17 cracks are noted within a line of $\sim 138\mu\text{m}$, resulting in a linear crack density of $0.123\mu\text{m}^{-1}$ for the $5\mu\text{L}$ and 30nM system. SEM image analysis gives a value $\sim 0.116\mu\text{m}^{-1}$ for the same.

The following table shows thickness of deposition of DNA-AuNP on the coffee ring measured by profilometer for samples of various volume and concentration.

Table S2: Coffee ring heights for various samples of different volume and concentration. Interestingly the formation of crack occur in case of samples with ring height $\geq 600nm$.

Volume (μL)	Concentration (nM)	Average ring height (nm)	Crack
2	2.5	328	No
2	5	600	Yes
2	15	940	Yes
4	2.5	797	Yes
4	20	2684	Yes
5	12.5	1508	Yes

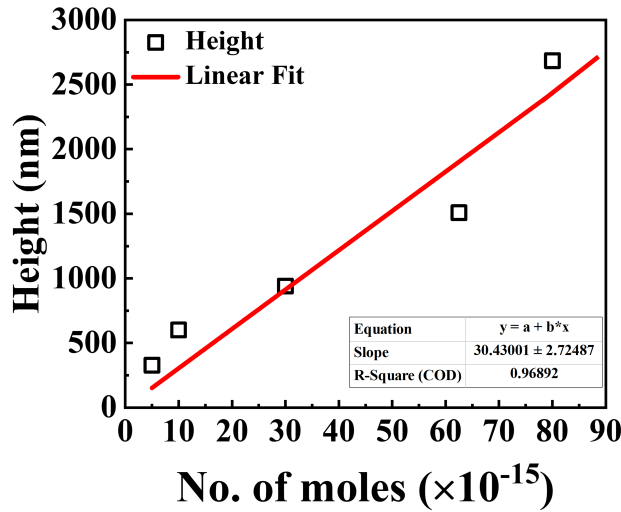


Fig. S7: Thickness of coffee ring/height of deposition vs number of particles (in moles). A linear profile shows the deposition thickness is precisely dependent on the total number of particles irrespective of concentration or volume.

Contact angle data

Initial contact angle values for different systems

The initial contact angle (θ_o) values for a $2\mu L$ DNA-AuNP droplet on SiO_2 surface with increasing concentration is shown. θ_o is taken to be independent of the concentration of DNA-AuNP as the trend suggests in Fig.S8.

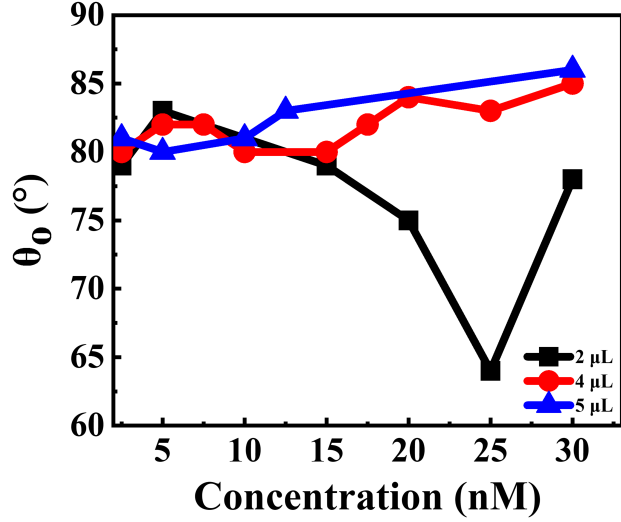


Fig. S8: Initial contact angle(θ_0) vs DNA-AuNP concentration for fixed volume of droplets.

Variation of t_{CCR} and t_{CCA} with nanoparticle concentrations and droplet volumes

The time spent by DNA-AuNP droplet in CCR mode (t_{CCR}) and CCA mode (t_{CCA}) of evaporation is shown here (Fig.S9) w.r.t nanoparticle concentrations and droplet volumes. The increase in t_{CCR} with concentration is very prominent as both t_{CCR} and t_{CCA} increases $\sim 1.5 - 2$ times when volume increases from 2 – 4 μL .

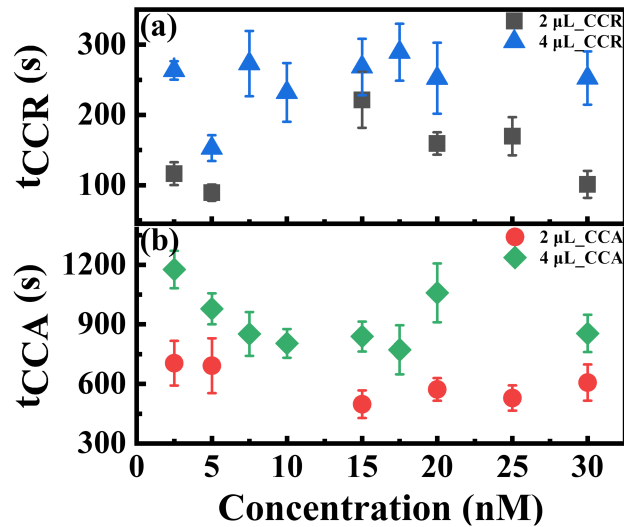


Fig. S9: t_{CCR} (a) and t_{CCA} (b) for a 2 μL and 4 μL droplet of various concentrations.

Fitting contact angle data

Contact angle variation with time is fitted using a piece-wise function as given in the following equations 1

$$\begin{aligned}
 y_{i1} &= a_1 + k_1 x_{i1}; \\
 y_{i2} &= y_{i1} + k_2(x_{i2} - x_{i1}); \\
 &\text{if}(x|x_{i1}) \\
 &y = a_1 + k_1 x; \\
 &\text{else if}(x|x_{i2}) \\
 &y = y_{i1} + k_2(x - x_{i1}); \\
 &\text{else} \\
 &y = y_{i2} + k_3(x - x_{i2});
 \end{aligned} \tag{1}$$

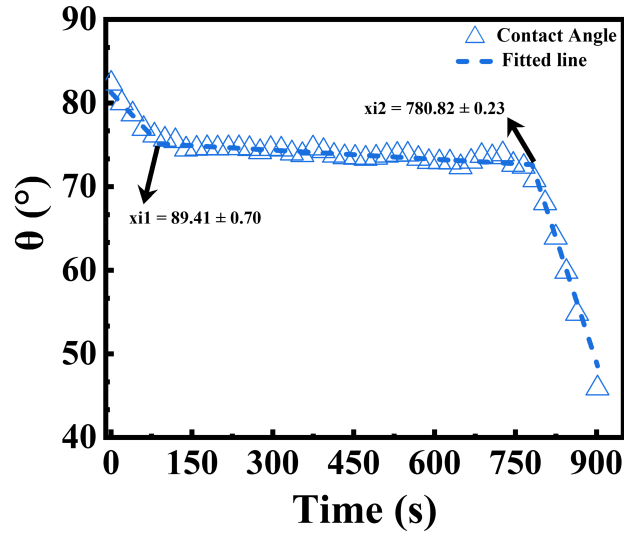


Fig. S10: Contact angle data and piece-wise fitting is shown here. The ends of *CCR* mode and *CCA* mode of evaporation is pointed as x_{i1} and x_{i2} .

The values of t_{CCR} and t_{CCA} from the fitted contact angle graph (S10) are calculated from the fitting parameters by the following equations 2

$$\begin{aligned}
 t_{CCR} &= x_{i1}; (t_0 = 0) \\
 t_{CCA} &= x_{i2} - x_{i1}
 \end{aligned} \tag{2}$$

Estimation for various interaction forces between the substrates and particles

Interaction forces between the DNA-AuNP and the substrates are estimated using the formulae given in literature.⁴ Here we are showing the van der Waals and electrostatic interaction between a particle and substrate as well as between two particles.

$$\text{van der Waals force between particle and substrate } (F_{WPS}) = \frac{2A_{132}R^3}{3z^2(z+2R)^2}$$

$$\text{Electrostatic force between particle and substrate } (F_{EPS}) = \frac{-2R\epsilon\kappa[\phi_1^2 + \phi_2^2 - 2\phi_1\phi_2\exp(kz)]}{\exp(2kz) - 1}$$

$$\text{van der Waals force between two particles } (F_{WPP}) = \frac{2A_{131}R}{12z_1^2}$$

$$\text{Electrostatic force between two particles } (F_{EPP}) = \frac{-2R\epsilon\kappa[\phi_1^2]}{\exp(kz_1) - 1}$$

Table S3: Estimates for various interaction forces amongst the substrates and particles

Force	Value (N)	Surface
F_{WPS}	$1.66 \times 10^{-14} N$	SiO_2
F_{WPP}	$1.95 \times 10^{-13} N$	SiO_2
F_{EPS}	$6.06 \times 10^{-20} N$	SiO_2
F_{EPP}	$1.4 \times 10^{-28} N$	SiO_2
F_{WPS}	$5.41 \times 10^{-11} N$	Si
F_{WPP}	$1.95 \times 10^{-13} N$	Si
F_{EPS}	$6.33 \times 10^{-12} N$	Si
F_{EPP}	$1.4 \times 10^{-28} N$	Si

The force values indicate equal particle-particle interaction in case of both the substrate which is expected. van der Waals attraction is higher in case of freshly cleaned Si substrate. As DNA is hydrophilic and the SiO_2 surface is comparatively hydrophobic, the attraction is lesser in that case.

Values of the parameters are given in the table S4 below.

Table S4: Estimates for various interaction forces amongst the substrates and particles. SI unit system is followed if not mentioned otherwise.

Parameter	Value
Contact angle (θ) for Si	12°
Contact angle (θ) for SiO_2	80°
Hamaker constant ($A_{Au,water,Si}$)	$4.92 \times 10^{-20\ 5-7}$
Hamaker constant ($A_{Au,water,SiO_2}$)	$3 \times 10^{-20\ 5,6,8}$
Hamaker constant ($A_{Au,water,Au}$)	$25 \times 10^{-20\ 5,6}$
Radius of particle (R)	$7.5nm$
Particle-substrate distance z (for Si)	$1nm$
Particle-substrate distance z (for SiO_2)	$20nm$
Particle-particle separation z_1	$40nm$
Debye length κ^{-1}	$1nm$
Permittivity of water ϵ	7×10^{-10}
Surface potential for DNA-AuNP (ϕ_1)	$-56mV$
Surface potential for Si/SiO_2 (ϕ_2)	$-25mV$
Water viscosity η	0.001
Water surface tension	$0.072N/m$
Water velocity v	$0.733\mu m/s^9$

References

- (1) Verhoeven, J. Glossary of terms used in photochemistry (IUPAC Recommendations 1996). *Pure and Applied Chemistry* **1996**, *68*, 2223–2286.
- (2) Li, D.; Neumann, A. Contact angles on hydrophobic solid surfaces and their interpretation. *Journal of colloid and interface science* **1992**, *148*, 190–200.
- (3) Li, D.; Neumann, A. Equation of state for interfacial tensions of solid-liquid systems. *Advances in Colloid and Interface Science* **1992**, *39*, 299–345.
- (4) Yu, Y.-S.; Wang, M.-C.; Huang, X. Evaporative deposition of polystyrene microparticles on PDMS surface. *Scientific reports* **2017**, *7*, 1–9.
- (5) Ederth, T. Computation of Lifshitz- van der Waals forces between alkylthiol monolayers on gold films. *Langmuir* **2001**, *17*, 3329–3340.

- (6) Israelachvili, J. N. *Intermolecular and surface forces*; Academic press, 2011.
- (7) Dahneke, B. The influence of flattening on the adhesion of particles. *Journal of Colloid and Interface Science* **1972**, *40*, 1–13.
- (8) Bergström, L. Hamaker constants of inorganic materials. *Advances in colloid and interface science* **1997**, *70*, 125–169.
- (9) Patil, N. D.; Bange, P. G.; Bhardwaj, R.; Sharma, A. Effects of substrate heating and wettability on evaporation dynamics and deposition patterns for a sessile water droplet containing colloidal particles. *Langmuir* **2016**, *32*, 11958–11972.